JOURNAL OF CATALYSIS 23, 168–182 (1971)

Hydrodemethylation of Toluene on Clinoptilolite

J. PAPP, D. KALLÓ, AND G. SCHAY

Central Research Institute for Chemistry, Hungarian Academy of Sciences, Budapest, Hungary

Received November 12, 1970

From kinetic studies of the catalytic hydrodemethylation of toluene on clinoptilolite exchanged by K^+, Mg^{2+}, and La^{3+} ions, respectively, the mechanism of the reaction could be deduced. The rate-determining step of the transformation is a surface reaction in which hydrogen from the gas phase reacts with chemisorbed toluene in a presumably four-center reaction resulting in gaseous methane and adsorbed benzene. The kinetic parameters of the reaction, i.e., the activation energies as well as the heats of adsorption of benzene or toluene are identical for all three catalysts, and suggest thus energetic homogeneity of the active sites. Possible active sites above 600°C are probably the strongly electrophilic Lewis centers, or ensembles of Lewis centers coupled with neighboring SiO_3^+ lattice groups. The presumption of such active formations is supported by the decrease of hydroxyl coverage and the high radical stabilizing power of the catalysts as proved by ESR measurements, and further by recognition of a linear relationship between the activity of the catalysts and their exchanged cation content. This correlation shows that bivalent or trivalent cations give rise to identical formations proportional in number to their equivalent amounts, the active sites formed being independent of the other properties of the respective cations.

INTRODUCTION

Both homogeneous and catalytic hydrodemethylation of toluene have been widely dealt with in the literature. In spite of this, the only point that seems firmly established is that homogeneous transformation is of first order with respect to toluene and of half order for hydrogen and that the reaction proceeds by a radical chain mechanism (*1–3*), but there are no generally valid statements even as to the apparent order of the catalytic reaction. Metals on supports (*4–7*), metal oxides (*4, 8, 9*) and insulators (*10, 11*) have been applied as catalysts, and it is, therefore, practically impossible to compare the results obtained by different authors. Using nickel on alumina as a catalyst under atmospheric pressure, Bazant *et al.*, for instance, arrived at the conclusion (*6*) simultaneously with us (*13*), that the surface reaction is the rate-determining step in which gaseous hydrogen reacts with adsorbed toluene. Notari and De Malde (*9*), on the other hand, assume that both toluene and hydrogen are chemisorbed on a chromia–alumina catalyst, the former under formation of benzyl radicals.

Although not yet verified, the general view is that the reaction proceeds by a radical mechanism on metals or semi-conducting metal oxides while on insulators the mechanism is ionic. The activation energy of the homogeneous reaction was found to be about 60 kcal/mole while that of the catalytic transformations ranged between 25–45 kcal/mole depending on the catalyst.

According to thermodynamic calculations, the equilibrium of the reaction

$$C_6H_5CH_3 + H_2 \rightarrow C_6H_6 + CH_4 \qquad (1)$$

is, in the temperature range of 600–660°C, entirely shifted towards the products while further hydrogenation processes conceivable in the toluene–hydrogen system, as, e.g., methylcyclohexane formation and total hydrocracking resulting in methane, are practically negligible.

The technical catalytic reaction is carried

out at several tens of atmospheres with hydrogen in considerable excess in order to suppress formation of carbonaceous deposits resulting in deactivation of the catalyst.

We have, therefore, carried out experiments at 80 atm total pressure of the hydrogen–toluene mixtures with hydrogen always in excess. The catalyst was a mineral, the main component of which is clinoptilolite. It has been found that the activity of this crystalline silica–alumina can be modified by ion exchange. The absence of aging when using these catalysts allowed a successful study of the mechanism of the hydrodemethylation of toluene.

Experimental

1. *Apparatus*

The reaction was carried out in an isothermal integral flow reactor. Toluene was fed continuously by a hydraulic micropump (capacity 1–10 ml/hr). The hydrogen was fed into the reactor from a high-pressure vessel through a valve system (intercept valve, fine regulator, and flap valve) and a thermistor microflow meter. After being preheated, the reaction mixture reached the desired temperature in the catalyst bed which was placed in the middle of the reactor where the temperature was kept constant within ±1°C. Temperature was measured with iron–constantan thermocouples and electric heating was regulated with a variable transformer. After being cooled the product passed through a gas–liquid separator. From here, both the gas and liquid passed through an expansion system. Analysis of the liquid product was made by gas chromatography using Griffin or Beckman apparatus with a thermal conductivity detector. The chromatograms were evaluated both quantitatively and qualitatively.

2. *Preparation and Description of the Catalysts*

A natural molecular sieve comprising about 70 vol % of clinoptilolite which, owing to its zeolitic character contains alkali and alkaline-earth ions together with a considerable amount of zeolitic water, has been found in Hungary. The remainder of about 30% is made up of an amorphous, vitreous component, besides quartz, cristobalite and feldspar identified by X-ray diffraction. The mineral was used as a catalyst after exchange of the mobile ions of the clinoptilolite component.

The clinoptilolite in this mineral was identified by Nemecz *et al.* (*12*). Although the exact structure of clinoptilolite is not yet established in all its details, it is known that its alumina–silica framework is isostructural with that of heulandite. By analogy, the unit cell is built up of 72 oxygen and 36 (silicon + aluminium) atoms. According to literary data, its approximate composition is: $Na_2O \cdot Al_2O_3 \cdot 10\ SiO_2 \cdot 8.6\ H_2O$, while that of the original clinoptilolite used in our experiments, as calculated from the OCl and DCl data of Table 1 is:

$$0.26\ K_2O \cdot 0.15\ MgO \cdot 0.59\ CaO \cdot 0.94\ Al_2O_3 \cdot 0.06\ Fe_2O_3 \cdot 10\ SiO_2 \cdot 6.7\ H_2O.$$

(OCl data refer to the composition of the original mineral, DCl to that after decationization; from the difference the composition of the zeolitic clinoptilolite component can be calculated.) The presence of trivalent aluminium (and ferric) ions leads to an excess negative charge which is then compensated by the cations present in the pores or cavities of the tetrahedral lattice. By exchange of the latter cations for other ions, the physical and chemical properties of clinoptilolite, mainly its pore size, adsorptive and catalytic properties can be altered without considerably reducing the heat stability of its crystal lattice, owing to the high silicon content. In order to alter systematically the catalytic activity of clinoptilolite, ions of different charge (K^+, Mg^{2+}, La^{3+}) were introduced by ion exchange (100 g of powdered material was treated twice, 2 hr each, with 400 ml of boiling 2 *M* aqueous solution of the respective nitrate and then washed with distilled water). The compositions of the different dehydrated ion-exchanged derivatives (catalysts K-30, Mg-1, La-1) as well as those of the natural mineral (OCl) and of the deca-

TABLE 1

COMPOSITION OF DIFFERENT CLINOPTILOLITE DERIVATIVES, DEHYDRATED AT 500°C

	OCl[a]			K-30[b]			Mg-1[c]			La-1[d]			DCl[e]		
Component	% by weight	Atom / atom Si	Eq / atom Si	% by weight	Atom / atom Si	Eq / atom Si	% by weight	Atom / atom Si	Eq / atom Si	% by weight	Atom / atom Si	Eq / atom Si	% by weight	Atom / atom Si	Eq / atom Si
SiO_2	77.15	Si:1		76.46	Si:1		77.83	Si:1		77.0	Si:1		81.58	Si:1	
Al_2O_3	12.25	Al:0.195		11.63	Al:0.179		12.54	Al:0.189		12.21	Al:0.187		13.27	Al:0.191	
Fe_2O_3	1.30	Fe:0.012		1.16	Fe:0.011		1.21	Fe:0.012		1.22	Fe:0.012		1.37	Fe:0.012	
Na_2O	0.48		0.012	0.47		0.012	0.49		0.012	0.40		0.011	0.42		0.010
K_2O	5.06		0.084	9.34		0.156	4.15		0.068	3.02		0.050	3.05		0.048
MgO	0.64		0.025	0.55		0.021	1.82		0.070	0.64		0.025	0.10		0.004
CaO	3.10		0.087	0.37		0.010	1.94		0.053	3.05		0.084	0.20		0.005
La_2O_3										2.45		0.035			
$\frac{\Sigma \text{ eq}}{\text{atom Si}}$			0.208			0.199			0.203			0.205			0.067

[a] OCl, original mineral.
[b] K-30, mobile ions exchanged for K^+.
[c] Mg-1, mobile ions exchanged for Mg^{2+}.
[d] La-1, mobile ions exchanged for La^{3+}.
[e] DCl, decationized by removal of the mobile cations.

TABLE 2

CONVERSIONS OF REACTION (1) ON CATALYST K-30; TOTAL PRESSURE 80 atm

Temp (°C)	$\left[\frac{\text{Mole}_H}{\text{mole}_T}\right]_{in}$[a]	$S^{-1} = 0.416 \times 10^3$		$S^{-1} = 0.83 \times 10^3$		$S^{-1} = 1.04 \times 10^3$		$S^{-1} = 1.39 \times 10^3$		$S^{-1} = 2.08 \times 10^3$		$S^{-1} = 4.16 \times 10^3$	
		(g_T^{-1} g_{cat} sec)											
		$Conv_T$ (mole %)	$n_T \times 10^{2}$[b]	$Conv_T$ (mole %)	$n_T \times 10^{2}$[b]	$Conv_T$ (mole %)	$n_T \times 10^{2}$[b]	$Conv_T$ (mole %)	$n_T \times 10^{2}$[b]	$Conv_T$ (mole %)	$n_T \times 10^{2}$[b]	$Conv_T$ (mole %)	$n_T \times 10^{2}$[b]
600	2:1	2	1.064	3	1.053	4	1.042	5	1.031	6	1.021	8	0.999
	3:1	2	1.064	4	1.042	4	1.042	5	1.031	7	1.010	8	0.999
	4:1	3	1.053	5	1.031	5	1.031	6	1.021	8	0.999	9	0.988
	5:1	3	1.053	5	1.031	6	1.021	6	1.021	8	0.999	11	0.966
620	2:1	3	1.053	3	1.053	4	1.042	6	1.021	7	1.010	8	0.999
	3:1	3	1.053	4	1.042	5	1.031	7	1.010	9	0.988	8	0.999
	4:1	3	1.053	6	1.021	7	1.010	7	1.010	9	0.988	10	0.977
	5:1	4	1.042	6	1.021	7	1.010	8	0.999	10	0.977	12	0.955
640	2:1	—	—	4	1.042	4	1.042	7	1.010	6	1.021	8	0.999
	3:1	—	—	5	1.031	5	1.031	7	1.010	8	0.999	9	0.988
	4:1	—	—	6	1.021	7	1.010	8	0.999	10	0.977	11	0.966
	5:1	—	—	8	0.999	7	0.988	11	0.966	12	0.955	13	0.944
660	2:1	5	1.031	7	1.010	8	0.999	9	0.988	12	0.955	16	0.912
	3:1	5	1.031	9	0.988	10	0.977	9	0.988	13	0.944	17	0.901
	4:1	7	1.010	9	0.988	10	0.977	10	0.977	13	0.944	18	0.889
	5:1	7	1.010	10	0.977	10	0.977	12	0.955	14	0.933	18	0.889

[a] T = toluene; H = hydrogen.

[b] $\text{Mole}_{T,out}$ $g_{T,in}^{-1}$.

tionized (DCl) form are summarized in Table 1.

As can be seen in Table 1, the sodium content remains practically unaltered in the different derivatives. It may be assumed that sodium is present in a fixed position in the nonclinoptilolite phase of the mineral; about 60% of the potassium, 5% of the calcium, and 15% of the magnesium content are similarly bound in fixed states.

The outer specific surface areas of the above clinoptilolite derivatives are practically identical: 25 m^2/g as calculated from adsorption isotherms of krypton at −196°C and 30 m^2/g from toluene adsorption isotherms at 104°C (*13*). These data are in good agreement with the value of 30 m^2/g given for clinoptilolite by Barrer, as derived from nitrogen adsorption isotherms at −196°C. It appears from these data that the elementary crystallite size is approximately 1000 Å. The real densities of our catalysts varied between 2.24 and 2.48 g/ml, while according to the literature, the density of pure clinoptilolite is 2.20 g/ml.

3. Kinetic Measurements

Before being taken into use, each catalyst sample was pretreated within the reactor by heating for 5 hours at the temperature of the actual experiment, in a 10 liters/hr stream of hydrogen.

Reaction (1) is exothermic and practically irreversible in the temperature range of the experiments. Conversions were measured under steady-state conditions at a total pressure of 80 atm, at 600, 620, 640, and 660°C, with hydrogen/toluene mole ratios of 2:1, 3:1, 4:1, 5:1, each at six different input rates (*15*). According to the material balance calculations, by-products could not have been formed to more than 0.5 wt %, which means that the reaction is quite straightforward. In order to obtain the true extent of catalytic transformation at each contact time, the conversions due to the homogeneous reaction were subtracted from the total transformations measured, taking into account the effective free volume of the reactor. Our reactor operated as an almost perfect tube-reactor material transport by longitudinal diffusion not exceeding 5% of the total flow. The catalytic activity did not change during any experiment, i.e., there was no difference between conversions measured under identical conditions at the beginning and at the end of each run. Two g of catalyst (grain size 1.0–1.25 mm) was the usual filling. Activity of the catalyst is not influenced by varying the grain size between 0.7 and 2.25 mm, showing that there is no hindrance by pore diffusion. This could be expected since the toluene molecules cannot penetrate into the micropores so that only the outer surface of the crystallites can be catalytically effective.

From the experimental data shown in Tables 2, 3, and 4, the so-called integral conversion curves have been plotted directly, see, e.g., the curves in Fig. 1 (La-1 catalyst at 660°C). The reaction rates may be directly obtained from the slopes of these curves in $\text{mole}_{\text{toluene}}\ g_{\text{cat}}^{-1}\ \text{sec}^{-1}$ units since the conversions are given as $\text{mole}_{\text{toluene,out}}/g_{\text{toluene,in}}$ and the reciprocal specific feed rates as $g_{\text{cat}}\ \text{sec}\ g_{\text{toluene,in}}^{-1}$.

The reaction rates determined in the above way form the basis of the following kinetic discussion.

Results

1. Selection of the Mechanism Compatible with the Kinetic Data

The elementary steps of the catalytic reaction of toluene with hydrogen may be supposed to satisfy either a Langmuir–Hinshelwood or a Rideal–Eley mechanism; in the sense of the former simultaneous chemisorption of toluene and of hydrogen (either in molecular or atomic form) has to be considered, followed by a surface reaction between the adsorbed components and the catalytic cycle is closed by the desorption of benzene and methane; while according to the latter mechanism, conversion is regarded to proceed via the adsorption of only one of the reactants, followed by the attack of the other reactant from the gas phase, resulting in one product molecule in the gaseous and one in the adsorbed state, which latter then desorbs (here also two types of hydrogen adsorption were taken into account). By assuming every

TABLE 3
CONVERSION OF REACTION (1) ON CATALYST Mg-1; TOTAL PRESSURE 80 atm

Temp (°C)	$\left[\frac{\text{Mole}_H}{\text{mole}_T}\right]_{in}$[a]	$S^{-1} = 0.416 \times 10^3$		$S^{-1} = 0.83 \times 10^3$		$S^{-1} = 1.04 \times 10^3$		$S^{-1} = 1.39 \times 10^3$		$S^{-1} = 2.08 \times 10^3$		$S^{-1} = 4.16 \times 10^3$	
		(g_T^{-1} g_{cat} sec)											
		$Conv_T$ (mole %)	$n_T \times 10^2$ [a]	$Conv_T$ (mole %)	$n_T \times 10^2$ [a]	$Conv_T$ (mole %)	$n_T \times 10^2$ [a]	$Conv_T$ (mole %)	$n_T \times 10^2$ [a]	$Conv_T$ (mole %)	$n_T \times 10^2$ [a]	$Conv_T$ (mole %)	$n_T \times 10^2$ [a]
600	2:1	2	1.064	5	1.031	6	1.021	6	1.021	8	0.999	10	0.977
	3:1	3	1.053	5	1.031	6	1.021	7	1.010	9	0.988	12	0.955
	4:1	3	1.053	6	1.021	7	1.010	7	1.010	10	0.977	12	0.955
	5:1	4	1.042	6	1.021	8	0.999	8	0.999	10	0.977	13	0.944
620	2:1	4	1.042	7	1.010	8	0.999	8	0.999	11	0.966	15	0.923
	3:1	5	1.031	7	1.010	9	0.988	10	0.977	11	0.966	16	0.912
	4:1	6	1.021	9	0.988	10	0.977	10	0.977	13	0.944	16	0.912
	5:1	7	1.010	10	0.977	10	0.977	12	0.955	13	0.944	17	0.901
640[b]	2:1	—	—	8	1.00	9	0.99	12	0.95	17	0.90	27	0.79
	3:1	—	—	9	0.99	10	0.98	14	0.93	18	0.89	27	0.79
	4:1	—	—	10	0.98	12	0.95	16	0.91	20	0.87	27	0.79
	5:1	—	—	12	0.95	15	0.92	17	0.90	21	0.86	27	0.79
660	2:1	9	0.988	14	0.933	16	0.912	19	0.879	23	0.836	28	0.781
	3:1	10	0.977	15	0.923	18	0.889	20	0.869	24	0.825	29	0.770
	4:1	10	0.977	16	0.912	19	0.879	22	0.847	25	0.814	29	0.770
	5:1	11	0.966	18	0.889	20	0.869	24	0.825	26	0.803	30	0.760

[a] $\text{Mole}_{T,out}$ $g_{T,in}^{-1}$.

[b] Reciprocal specific feed rates S^{-1} are —, 0.73×10^3, 0.90×10^3, 1.23×10^3, 1.82×10^3, 3.70×10^3 g_T^{-1} g_{cat} sec.

TABLE 4

CONVERSION OF REACTION (1) ON CATALYST La-1; TOTAL PRESSURE 80 atm

Temp (°C)	$\left[\frac{\text{Mole}_H}{\text{mole}_T}\right]_{in}$	$S^{-1} = 0.416 \times 10^3$		$S^{-1} = 0.83 \times 10^3$		$S^{-1} = 1.04 \times 10^3$		$S^{-1} = 1.39 \times 10^3$		$S^{-1} = 2.08 \times 10^3$		$S^{-1} = 4.16 \times 10^3$	
		(g_T^{-1} g_{cat} sec)											
		$Conv_T$ (mole %)	$n_T \times 10^2$ [a]	$Conv_T$ (mole %)	$n_T \times 10^2$ [a]	$Conv_T$ (mole %)	$n_T \times 10^2$ [a]	$Conv_T$ (mole %)	$n_T \times 10^2$ [a]	$Conv_T$ (mole %)	$n_T \times 10^2$ [a]	$Conv_T$ (mole %)	$n_T \times 10^2$
600	2:1	3	1.053	4	1.042	6	1.021	6	1.021	8	0.999	10	0.977
	3:1	4	1.042	5	1.031	6	1.021	7	1.010	9	0.988	12	0.955
	4:1	4	1.042	5	1.031	7	1.010	7	1.010	10	0.977	13	0.944
	5:1	4	1.042	6	1.021	7	1.010	8	0.999	11	0.966	13	0.944
620	2:1	4	1.042	7	1.010	7	1.010	9	0.988	11	0.966	15	0.923
	3:1	5	1.031	8	0.999	9	0.988	9	0.988	12	0.955	16	0.912
	4:1	5	1.031	9	0.988	10	0.977	10	0.977	12	0.955	17	0.901
	5:1	6	1.021	10	0.977	10	0.977	11	0.966	14	0.933	17	0.901
640	2:1	5	1.031	10	0.977	12	0.955	12	0.955	18	0.889	25	0.814
	3:1	6	1.021	11	0.966	13	0.944	16	0.912	19	0.879	26	0.803
	4:1	7	1.010	12	0.955	15	0.923	16	0.912	22	0.847	26	0.803
	5:1	7	1.010	14	0.933	15	0.923	18	0.889	23	0.836	27	0.792
660	2:1	8	0.999	16	0.912	18	0.889	19	0.879	24	0.825	28	0.781
	3:1	10	0.977	16	0.912	19	0.879	21	0.858	25	0.814	28	0.781
	4:1	10	0.977	17	0.901	19	0.879	22	0.847	25	0.814	30	0.760
	5:1	12	0.955	17	0.901	21	0.858	23	0.836	27	0.792	30	0.760

[a] $\text{Mole}_{T,out}$ $g_{T,in}^{-1}$.

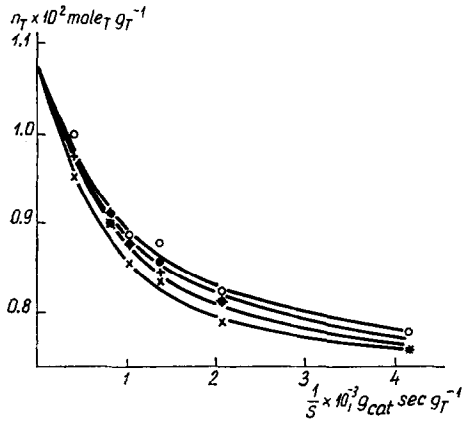

FIG. 1. Conversion curves of reaction (1) on catalyst La-1 at 660°C; total pressure 80 atm; mole ratio of hydrogen to toluene in the feed 5:1 (×), 4:1 (+), 3:1 (●), and 2:1 (○).

time one particular step as rate controlling, 26 different tentative mechanisms and corresponding rate equations were set up for the case of homogeneous active sites (as prompted by the uniformity of the crystal structure). The compatibility of any one of these kinetic equations could easily be checked graphically by rearranging them in a way that their respective right-hand sides should be linear functions of the partial pressures.

Provided, e.g., that toluene adsorption is rate controlling, the kinetic equations are in the Langmuir–Hinshelwood case as follows:

(a) For molecular hydrogen adsorption,

$$W = k \frac{p_T}{1 + K_H p_H + K_B p_B + K_M p_M}; \quad (2)$$

(b) for atomic hydrogen adsorption,

$$W = k \frac{p_T}{1 + \sqrt{K_H p_H} + K_B p_B + K_M p_M}, \quad (3)$$

where

W is the reaction rate, in $mole_T\ g_{cat}^{-1}\ sec^{-1}$;

k is the rate constant, in $mole_T\ g_{cat}^{-1}\ sec^{-1}\ atm^{-1}$;

K is the adsorption equilibrium constant, in atm^{-1};

p is the partial pressure, in atm; and the subscripts T, H, B, and M refer to toluene, hydrogen, benzene, methane, respectively,

while in case of the Rideal–Eley mechanism:

$$W = k \frac{p_T}{1 + K_B p_B}, \quad (4)$$

or

$$W = k \frac{p_T}{1 + K_M p_M}. \quad (5)$$

According to these kinetic equations, p_T/W plotted as a function of the corresponding partial pressures should give straight lines with positive slopes. This is, however, not borne out by experiment as may be seen, e.g., from Figs. 2 and 3 so that toluene adsorption cannot be considered as the rate-controlling step.

Desorption of one or the other of the products can simply be excluded as rate-controlling step, for W should then be independent of partial pressures, the total reaction being irreversible, but this conclusion is in contradiction with the experimental findings (cf. Fig. 1).

Without going into further details, it can be stated that from the 26 alternatives mentioned above, only the following has been found compatible with our experimental results: first-step fast adsorption of toluene, second and slow rate-determining step (rate constant k) reaction of hydrogen from the gas phase with adsorbed toluene followed

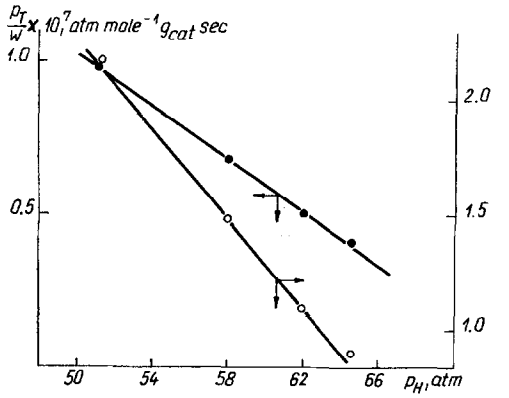

FIG. 2. Check of the linearized kinetic Eq. (2) on catalyst La-1 at 660°C (●) and on catalyst Mg-1 at 640°C (○); benzene partial pressure: 2 atm.

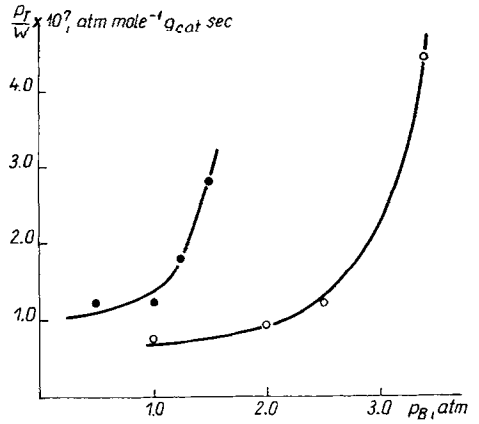

FIG. 3. Check of the linearized kinetic Eqs. (4) and (5) on catalyst K-30 at 660°C (●) and on catalyst Mg-1 at 640°C (○); mole ratio of hydrogen to toluene 5:1.

finally by fast desorption of adsorbed benzene or possibly adsorbed methane. Methane adsorption can be, however, disregarded as it is highly improbable that adsorbed toluene should result in adsorbed methane instead of adsorbed benzene. The according kinetic equation is:

$$W = kK_T \frac{p_T p_H}{1 + K_B p_B + K_T p_T}, \qquad (6)$$

where K_B and K_T are the respective adsorption equilibrium constants of benzene and toluene, or in linearized form:

$$\frac{p_T p_H}{W} = a + b p_B + c p_T. \qquad (7)$$

Plots of the left-hand side of the latter expression at constant p_B or p_T, respectively, proved linear in fact, with positive slopes and intercepts as required.

2. *Kinetic Constants and Their Temperature Dependence*

The experimental results point to an identical reaction mechanism on all three clinoptilolite derivatives in the temperature range studied and to this mechanism being adequately represented by the kinetic Eq. (6). Thus, by determining graphically the constants a, b, and c in the linearized Eq. (7), the respective true rate and equilibrium constants can be calculated as follows: $1/c = k$, mole g_{cat}^{-1} sec^{-1} atm^{-1}; $b/a = K_B$, atm^{-1}, $c/a = K_T$, atm^{-1}. An example of the representation suitable for such calculations is shown in Fig. 4: The slope of the parallel straight lines belonging to different values of p_B is c, their respective intercepts are $(a + bp_B)$, from which a and b can be calculated. The values a, b, and c obtained on all three catalysts at the four temperatures of the experiments together with the calculated values of k, K_B, and K_T are given in Table 5.

The temperature dependence of the rate constants gives an identical value of 43 ± 2 kcal/mole on all three catalysts for the activation energy of the rate-determining surface reaction (see Fig. 5). On the other hand, the pre-exponential factor is the highest for La-1, somewhat lower for Mg-1, and much lower for K-30, which may be due to a decrease in number of catalytically active sites. The identical slopes of the Arrhenius plots of the adsorption equilibrium constants also confirm that the active centers are energetically equivalent (see Figs. 6 and 7). Differences in absolute values, as revealed by Figs. 6 and 7, may probably be due to differences in adsorption entropy, the exact interpretation of which presents a problem not only in the given case but in general, too.

The accuracy of determination of the adsorption constants is very poor because,

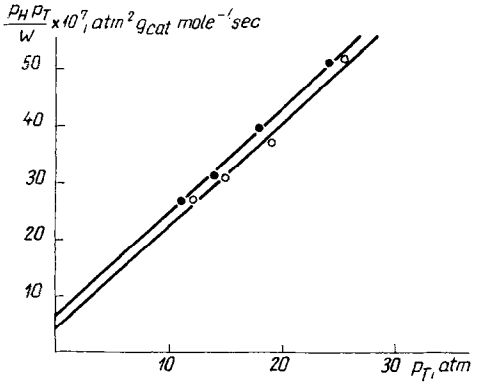

FIG. 4. Check of rate Eq. (7) on catalyst La-1 at 660°C; benzene partial pressure: 1.0 (○) and 2.0 atm (●).

TABLE 5

CONSTANTS a, b, AND c OF EQ. (6), RATE CONSTANTS k, ADSORPTION EQUILIBRIUM CONSTANTS OF BENZENE AND TOLUENE, K_B AND K_T, RESPECTIVELY, FOR THE CATALYSTS K-30, Mg-1, AND La-1

Cat	Temp (°C)	$a \times 10^{-7}$ 1[a]	$b \times 10^{-7}$ 2[b]	$c \times 10^{-7}$ 3[c]	$k \times 10^7$ mole g_{cat}^{-1} sec^{-1} atm^{-1}	K_B (atm^{-1})	K_T (atm^{-1})
K-30	600	7	22	21.70	0.046	3.14	3.10
	620	7	20	13.00	0.077	2.86	1.86
	640	7	10	7.20	0.139	1.43	1.03
	660	6	14	5.45	0.183	2.33(?)	0.91
Mg-1	600	3	16	9.90	0.101	5.33	3.33
	620	3	10	5.65	0.177	3.33	1.88
	640	5	7	3.70	0.270	1.40	0.74
	660	2.5	2.5	1.85	0.540	1.00	0.74
La-1	600	2	16	9.20	0.109	8.00	4.60
	620	2	10	4.80	0.208	5.00	2.40
	640	2	5	4.10	0.244	2.50	2.05
	660	2	2	1.80	0.555	1.00	0.90

[a] Number 1, $a \times 10^{-7}$ ($mole^{-1}$ g_{cat} sec atm^2).
[b] Number 2, $b \times 10^{-7}$ ($mole^{-1}$ g_{cat} sec atm).
[c] Number 3, $c \times 10^{-7}$ ($mole^{-1}$ g_{cat} sec atm).

on the one hand, their calculation has been based essentially upon intercepts extrapolated to $p_T = 0$ and on the other hand, the relatively small benzene partial pressures cannot be evaluated except with a considerable error. In spite of this inaccuracy, Figs. 6 and 7 indicate an exothermic heat of chemisorption of 40–60 kcal/mole for toluene as well as for benzene.

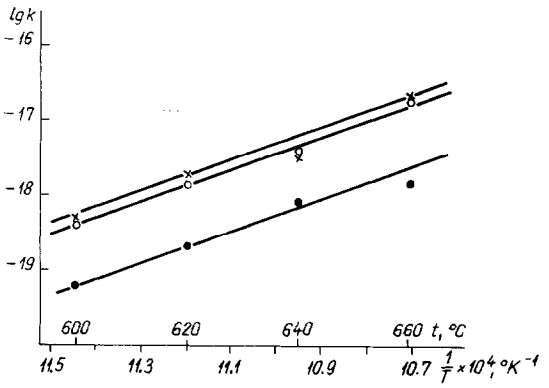

FIG. 5. Temperature dependence of the rate constants found on clinoptilolite catalysts exchanged with K^+ (●), Mg^{2+} (○), and La^{3+} (×) ions.

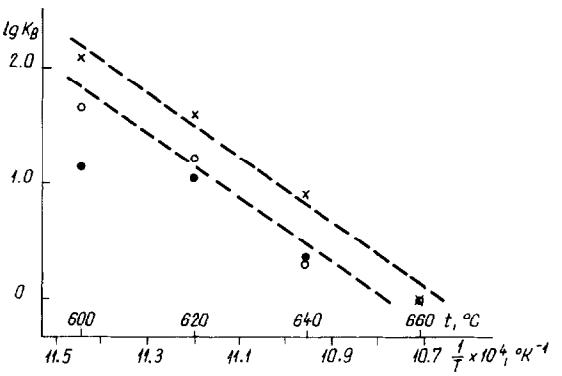

FIG. 6. Temperature dependence of the adsorption constant of benzene on catalysts K-30 (●), Mg-1 (○), and La-1 (×).

DISCUSSION

1. *Correlation Between Catalyst Composition, Structure, and Kinetic Parameters of the Reaction*

Our experimental results seem to throw light on the mechanism by which the clinoptilolite catalysts exert their effect. There exist several studies of the problem of how the activity of zeolite type catalysts

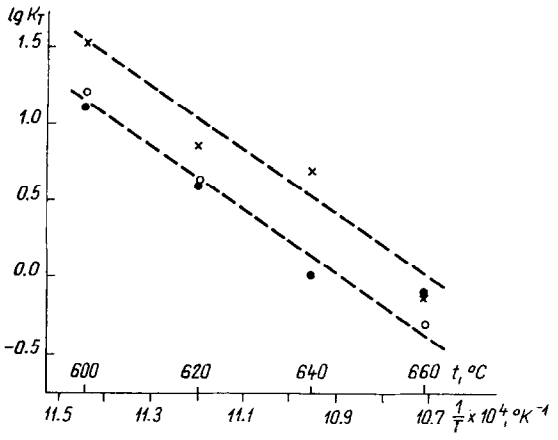

FIG. 7. Temperature dependence of the adsorption constant of toluene on catalysts K-30 (●), Mg-1 (○), and La-1 (×).

with surface hydroxyl groups is affected by water and incorporated cations (*16–20, 23*). Active Brönsted-type acidic groups transform above ~550°C into Lewis centers owing to dehydroxylation. This kind of transformation is practically completed at the temperatures of our experiments. We could not find, however, any reference in the literature as to the structure of the catalytically active sites thus formed, nor to the effect exerted upon them by cations, i.e., to the question of what detailed catalytic mechanism may be attributed to the surface formations present at such high temperatures.

Our kinetic results show that the reaction proceeds by an identical mechanism on clinoptilolite catalysts with their mobile ions exchanged in different ways. The values of the activation energies as well as the heats of adsorption of benzene and toluene also proved to be identical on all three catalysts. This leads to the conclusion that all the active formations are energetically equivalent, which points presumably to their structures being identical.

The changes in the number of surface hydroxyl groups as a function of temperature were investigated by ESR. ESR spectra

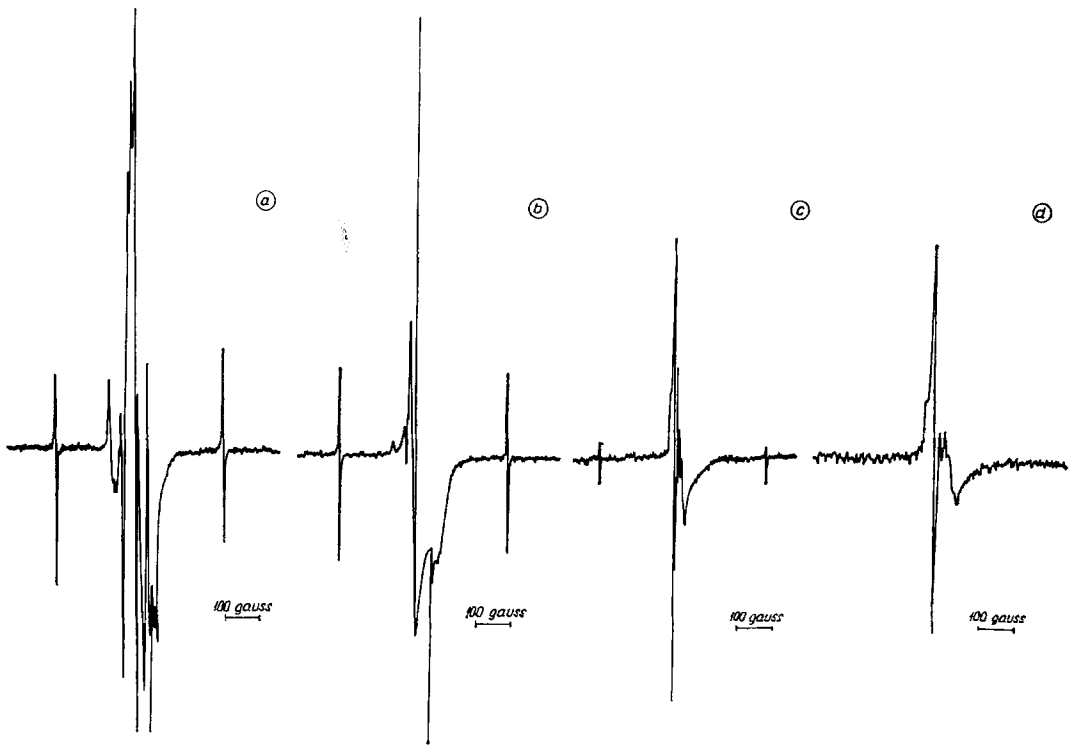

FIG. 8. ESR spectra of La-1 catalysts at −196°C; the samples were pretreated *in vacuo* at 400 (a), 500 (b). 600 (c), and 700°C (d).

determined at −196°C at $\lambda = 3.2$ cm wavelength of La-1 catalyst samples pretreated *in vacuo* at different temperatures (400, 500, 600, and 700°C) then irradiated by γ-rays, are shown in Fig. 8. Upon γ-irradiation, H atoms are formed from the hydroxyl groups whose doublet appears in Fig. 8 to the right and left of the complicated central signal. Comparison of Figs. 8(a), (b), (c), and (d), shows that the hydroxyl coverage does not change essentially up to 500°C, while at 600°C there is a sharp decrease, and at 700°C the surface becomes free of hydroxyls. ESR spectra of the catalysts K-30 and Mg-1 follow the same pattern.

These experimental results and literary data (*19*, *20*) point to the presence of the following formations of active sites on a clinoptilolite catalyst above 600°C: (a) in the absence of mobile cations

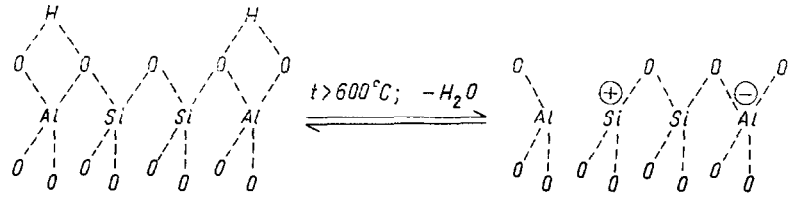

(b) in the presence of some multivalent cation (e.g., Mg^{2+})

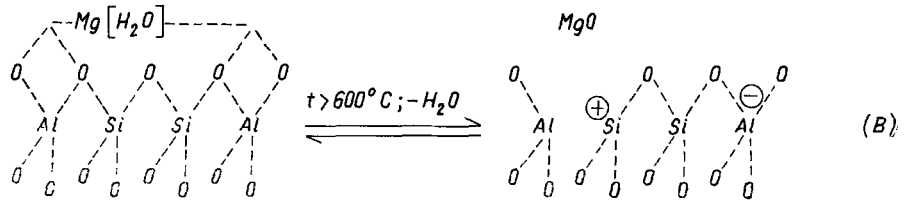

Similar to (b), three active sites are formed in the environment of two trivalent cations (dehydration–dehydroxylation cannot occur with monovalent cation substitution).

It follows that Brönsted sites cannot be involved in the reaction above 600°C, and the energetic homogeneity of the catalytic centers is not really surprising if the above surface structures A and B are considered.

It can be shown that catalytic activity is correlated to the above structural formation. Catalytic activities may be compared on the basis of the rate constants k_i (i meaning K-30, Mg-1, La-1, respectively) at any selected temperature or better characterized by the relative values ${}^*k_{i,0}$ of their pre-exponential factors which are: 2.24 for Mg-1 and 2.63 for La-1 when taking ${}^*k_{\text{K-30},0} = 1.00$. Further, if the active sites of the different catalysts are energetically identical, the activities related to a single active site should also be identical, i.e., ${}^*k'_0 = {}^*k_{i,0}/N_i$ (where N_i is the number of active centers in 1 g of catalyst; ${}^*k'_0$ is the pre-exponential factor of the rate constant referred to a single active site) should have the same value for all catalysts. In other words, we have to find appropriate values of N_i (or values proportional to N_i) which reduce the different ${}^*k_{i,0}$ (or either the k_i) to a common value.

On the basis of the foregoing structural considerations, we may try to set N_i proportional to the number of exchangeable bivalent cations and one and half the number of trivalent cations, both referred to 1 atom Si, but we obtain then different values for ${}^*k_{i,0}/N_i$. Plotting, however, ${}^*k_{i,0}$ as a function of the exchangeable potassium content, i.e., of the potassium content present in the clinoptilolite phase, denoted $(K^+)_{cl}$, there results a quite satisfactory linear correlation represented by the straight line II in Fig. 9. It is evident from the figure that the catalyst will possess some so-called residual activity even after maximal ion exchange, i.e., on introducing 134 ± 1 meq K^+/g-atom silicon (see the value marked $\frac{1}{0}$ in Fig. 9).

Presumably this residual activity may be

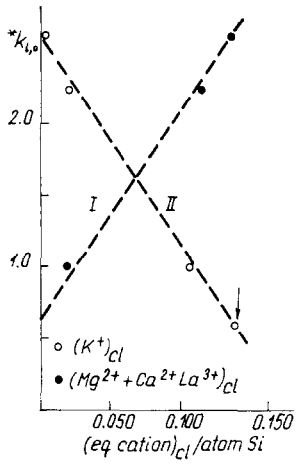

FIG. 9. Catalytic activity as a function of cation concentrations $(K^+)_{cl}$ (○) and $(Mg^{2+} + Ca^{2+} + La^{3+})_{cl}$ (●).

ascribed to formation A (see above) since removal of the hydroxyl groups initially present on the catalyst will result in formations identical with the active centers generated by bi and trivalent cations.

From the ion-exchanging properties of the catalyst there follows the stoichiometric equation

$$\text{const} - (K^+)_{cl} = \left(\frac{Mg^{2+} + Ca^{2+}}{2} + \frac{La^{3+}}{3}\right)_{cl} \equiv (\text{Me}) \text{ eq/atom Si} \quad (8)$$

for the cation equivalents referred to the silicon content, thus the $^*k_{i,0}$ values lie on a straight line (line I in Fig. 9) with a course opposite to II. It should be noted that k_i values pertaining to a given temperature, plotted in this manner, lie also on a straight line and that the few rate constants which we have determined on natural and decationized (OCl and DCl in Table 1) clinoptilolite catalysts, respectively, fit completely into the sequence.

Straight line I in Fig. 9 can be represented by the following equation:

$$^*k_{i,0} = 14.5\ (\text{Me}) + 0.60, \quad (9)$$

where (Me) is given by Eq. (8) and the intercept 0.60 represents the so-called remanent activity, when (Me) = 0.

Rearranging Eq. (9), we obtain

$$^*k_0'' = 14.5 = \frac{^*k_{i,0}}{(\text{Me}) + 0.041}, \quad (10)$$

where 0.041 is the number of active sites responsible for the residual activity per 1 atom of silicon. Substitution of the respective (Me) cation concentrations in Eq. (10) gives

$$\frac{1}{0.063} = 15.8; \frac{2.24}{0.155} = 14.4; \frac{2.62}{0.175} = 15.0$$

for the $^*k_0''$ values of K-30, Mg-1, and La-1 catalysts, respectively. The fair agreement of these three values is another expression of the linear relationship revealed by Fig. 9.

It appears thus confirmed that catalytically active sites are generated in a number proportional to the equivalent amounts of bi and trivalent cations introduced by ion exchange; the active sites thus formed are all equivalent and thus independent of the other properties of the cations (ionic radius, electrostatic potential, etc.). The catalysts bear, on the other hand, additional active formations A which are predominant in the case of exchange by K^+ ions. Validity of Eq. (10) as well as the identity of the activation energies proves the equivalence of the active formations A and B illustrated above.

2. The Micromechanism of the Reaction

Our kinetic results show that the rate-determining step of the hydrodemethylation of toluene on clinoptilolite is the irreversible reaction between adsorbed toluene and a hydrogen molecule attacking from the gas phase. The study of the catalysts led to the conclusion that the active catalyst formations comprise a nucleophilic (AlO_4^-) and two vicinal electrophilic (SiO_3^+; AlO_3) groups. The electron octet of the former is complete and the configuration is sterically shielded while the latter two have an electron sextet and are sterically more accessible; it is thus certainly the latter two which participate in the catalytic process.

The electrophilic character of the catalysts, i.e., their extraordinarily strong electron affinity, has been experimentally proven. The ESR investigations made in connection with the hydroxyl coverage

revealed an unusually strong radical stabilizing effect in clinoptilolite catalyst samples pretreated above 600°C (*21*): The adsorbed hydrogen atoms generated by γ-irradiation from hydroxyl groups were observable for several hours even at room temperature.

A similarly strong radical stabilizing effect could be detected for methyl radicals formed by the catalytic decomposition of diisobutyl peroxide as well as for ethyl and methyl radicals generated by radiolysis of ethyl and methyl bromide, respectively. These effects have to be ascribed to a strong single electron bond which may be attributed to the high electron affinity of the catalyst.

The electronic characteristics of the reactants and products, such as ionization potentials and molar polarizations, together with the strong electrophilic effect of the catalysts suggest, in agreement with our kinetic results, that the catalysts will interact strongly with toluene or benzene, resulting in the chemisorption of the latter. The high rates of chemisorption of toluene and benzene are probably due to the fact that only one electron has to be shifted or transmitted in the process. It is the benzene ring naturally which has to be made responsible for this property so that the toluene molecule adsorbs probably by insertion of the ring plane between the two electrophilic groups of the catalyst:

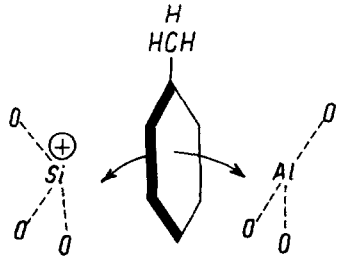

In this configuration the electron system of the benzene ring can be easily "pumped off" perpendicular to its plane. Owing to electron suction, the $C_{aromatic}$–C_{methyl} bond weakens: the electron system of the benzene ring tends to reassure its original structure and this completion entails a shift of the binding electrons.

According to our assumption, the hydrogen molecule coming from the gas phase attacks the loosened group, i.e., the polarized toluene molecule, in a four-center reaction. In this configuration, polarization simultaneously facilitates the dissociation of the hydrogen molecule, resulting in an adsorbed molecule of benzene and one of methane going immediately into the gas phase (*22*).

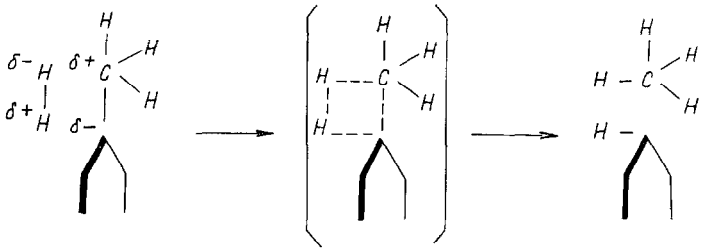

Owing to the escape of the methane, this process is naturally irreversible and thus meets the kinetic requirement that the rate-determining surface reaction should be irreversible. The catalytic cycle is closed by a fast desorption of benzene.

It may also be assumed, as an extreme case of the above mechanism, that the loosened methyl group splits off as a radical, leaving a phenyl cation or, by readmission of the electron from the catalyst to the aromatic system, a phenyl radical on the surface. Collision in the gas phase between a hydrogen molecule and the methyl radical leads to the formation of methane and a hydrogen atom. The latter had to react immediately with the adsorbed phenyl cation (or phenyl radical) in order that the reaction cycle should be completed in accordance with the correct kinetic equation. The collision probability for the latter step is, however, very slight, and thus, though a radical ionic or radical rearrangement cannot be definitely excluded on the basis of our results, it may be regarded as an improbable extreme case.

Further investigations of the catalyst

transformations and of the electronic character of the catalysts were initiated by the kinetic study outlined here.

Acknowledgments

The authors wish to thank Prof. Dr. I. Náray-Szabó and Dr. A. Messmer for their helpful discussions.

References

1. Silsby, R. J., and Sawyer, E. W., *J. Appl. Chem.* **6**, 347 (1956).
2. Betts, B. D., Popper, F., and Silsby, R. J., *J. Appl. Chem.* **7**, 497 (1957).
3. Matsui, H., Amano, A., and Tokuhisa, H., *Bull. Jap. Petrol. Inst.* **1**, 67 (1959).
4. Doumano, T. B., *Ind. Eng. Chem.* **50**, 1677 (1958).
5. Seeboth, H., and Rieche, A., *Brennst. Chem.* **46**, 36e (1965).
6. Setinek, K., Pecev, N., and Bazant, B., *Collect. Czech. Chem. Commun.* **33**, 1451 (1968).
7. Shuikin, N. I., Berdnikova, N. G., and Kaskovskaya, L. K., *Izv. Akad. Nauk SSSR*, 308 (1959).
8. Weiss, H. A., and Friedman, L., *Ind. Eng. Chem. Process Des. Develop.* **2**, 193 (1963).
9. Notari, B., Duranti, V. P., and De Maldé. M., *Proc. Int. Congr. Catal., 3rd (1964)* **2**, 1034 (1965).
10. Mamedaliev, J. G., *Dokl. Akad. Nauk SSSR* **106**, 1027 (1956).
11. Kazanskii, B. A., and Georgiev, H. D., *Dokl. Akad. Nauk SSSR* **116**, 85 (1957).
12. Nemecz, E., and Varju, Gy., *Földt. Közl. Agyagásvány Füz.* **93**, 77 (1963).
13. Papp, J., and Kalló, D., *Magy. Kém. Foly.* **75**, 99 (1969).
14. Barrer, R. M., Papadopoulos, R., and Rees, L. V. C., *J. Inorg. Nucl. Chem.* **29**, 2047 (1967).
15. Papp, J., and Kalló, D., *Magy. Kém. Foly.* **76**, 617 (1970).
16. Pickert, P. E., Rabó, J. A., Dempsey, E., and Schomaker, V., *Proc. Int. Congr. Catal. 3rd (1964)* **1**, 714 (1965).
17. Frilette, V. J., and Weisz, P. B., *J. Phys. Chem.* **64**, 382 (1960).
18. Agudo, A. L., Badcock, F. R., and Stone, F. S., *Proc. Int. Congr. Catal. 4th (1968)*, prepr. 59 (1969).
19. Uytterhoeven, J. B., Christner, L. G., and Hall, W. K., *J. Phys. Chem.* **69**, 2117 (1965).
20. Hughes, T. R., and White, H. M., *J. Phys. Chem.* **71**, 2192 (1967).
21. Papp, J., Miheikin, I. D., and Kazanszkii, V. B., *Kinet. Katal.* **11**, 812 (1970).
22. Papp, J., and Kalló, D., *Magy. Kém. Foly.* **77**, 104 (1971).
23. Ward, J. W., *J. Catal.* **9**, 225 (1967); **10**, 34 (1968); **11**, 251 (1968).